BBAA VI International Colloquium on:
Bluff Bodies Aerodynamics & Applications
Milano, Italy, July, 20-24 2008

NON-STATIONARY TORNADO-INDUCED WIND LOADS COMPARED WITH TRADITIONAL BOUNDARY LAYER WIND LOADS ON LOW-RISE BUILDINGS

Fred L. Haan, Jr.[*], Partha P. Sarkar[*], Vasanth K. Balaramudu[*]

[*]Department of Aerospace Engineering
Iowa State University, Ames, Iowa, 50011 U.S.A.
e-mail: haan@iastate.edu, ppsarkar@iastate.edu, vasanth@iastate.edu, weizhang@iastate.edu

Keywords: low-rise buildings, bluff body aerodynamics, tornado, non-stationary events.

Abstract. *The effects of wind loading on buildings due to straight line boundary layer type winds have been studied extensively in the past. Building code provisions are based primarily on studies of this sort. Comparatively little research has been done, however, to study how buildings and other structures are affected by transient, non-stationary, three-dimensional flow phenomena such as tornadoes. This paper summarizes data from an investigation of the effects of tornado-induced wind loading on low-rise buildings. Extensive testing was performed on low-rise building models (1:100) to compare the loading patterns resulting from the tornado-like vortices of a large laboratory tornado simulator to ASCE 7-05 provisions. It was found that lower vortex translation speeds resulted in larger peak force magnitudes. It was also found that tornadoes of smaller diameter produced larger peak forces. While* $C_{\hat{F}_x}$ *and* $C_{\hat{F}_y}$ *showed some dependence on building orientation with respect to the tornado translation axis,* $C_{\hat{F}_z}$ *exhibited no significant dependence of this type.*

1 INTRODUCTION

This paper summarizes the results of the use of a laboratory tornado simulator to quantify tornado-induced wind loading on low-rise building models. With a single building model, a range of tornado sizes was tested. With a single tornado, a range of building geometries was tested. This paper describes the experimental approach, the general character of the tornado-induced loading and the results of the extensive building model tests.

2 EXPERIMENTAL APPROACH

The tornado simulator at Iowa State University was used for these experiments (see Fig. (1)). The tornado simulator consists of a circular duct 5.49 m in diameter and 3.35 m high is suspended from a 4500 kg overhead crane so that it can translate along a 10.4m long ground plane. A 1.83m diameter fan is mounted in the center of this duct to act as an updraft. The maximum translation speed of the crane is 0.61 m/s. More details on the design and validation of this system can be found in Ref. [1]. By adjusting the amount of inflow rotation, a range of vortex diameters and vortex flow patterns were generated (with swirl ratios ranging from 0.08 to 1.14). Using an 18-hole pressure probe, the tornado flow fields were measured and found to agree well with Doppler radar data from the Spencer, South Dakota tornado of 1998 and the Mulhall, Oklahoma tornado of 1999 (from Ref. [2]).

A single-story, gable roof building model (nominally 1:100 scale with a 91mm by 91mm plan, an eave height of 36mm, gable roof angle of 35° and maximum height of 66 mm) was subjected to the facility's full range of tornado sizes, types and translation speeds. Additional tests were performed on similarly-scaled buildings to observe effects of building height and roof geometry. The roofs that were tested included: a flat roof, a hip roof with 15° degree angle and gable roofs with 15°, 25° and 35° angles. Pressure and force measurements were conducted using a Scanivalve electronic pressure scanner and a 6-component load cell, respectively. The force measurements were conducted only on a select few cases as a check on accuracy. The results presented in this paper were all derived from pressure measurements.

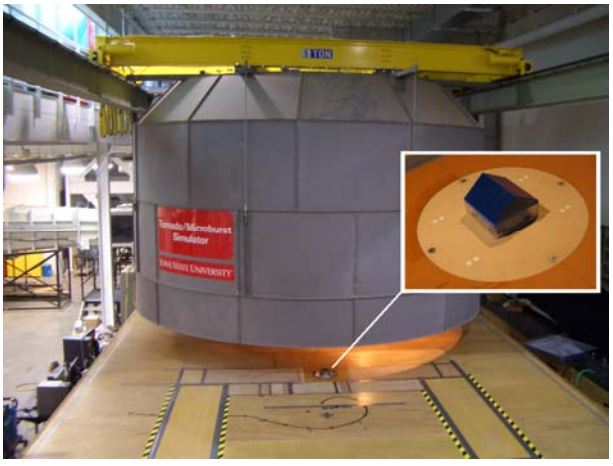

Figure 1: Photo of the tornado simulator at Iowa State University.

3 GENERAL CHARACTER OF THE TORNADO-INDUCED WIND LOADING

Overall forces on the models were quantified by integrating the external pressure distributions. Internal pressures were not modeled. Aerodynamic forces were normalized according to Eq. (1) with the average, maximum tangential velocity from the vortex core, $V_{\theta_{\max}}$, and with areas, *S*, shown in Fig. (1).

$$C_{F_x} = \frac{F_x}{\frac{1}{2}\rho V_{\theta_{\max}}^2 S_x} \quad C_{F_y} = \frac{F_y}{\frac{1}{2}\rho V_{\theta_{\max}}^2 S_y} \quad C_{F_z} = \frac{F_z}{\frac{1}{2}\rho V_{\theta_{\max}}^2 S_z} \tag{1}$$

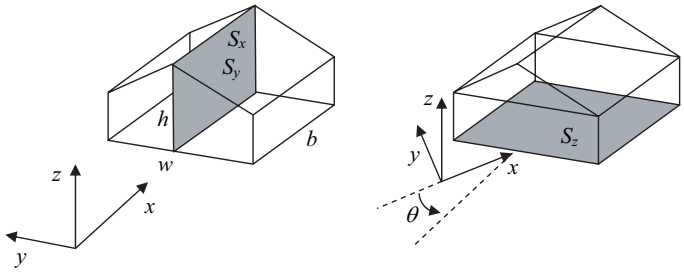

Figure 1: Illustration showing the building orientation with respect to the vortex translation direction (*x*-axis).

Fig. (2) shows a figure representative of the forces on the building models as the tornado vortex passes. The variable *x* represents the position of the vortex with respect to the center of the building. The tornado moves in the positive *x* direction. $C_{\hat{F}_x}$ shows the tornado drawing the building toward itself as it approaches from the negative *x*-direction and as it leaves in the positive *x*-direction. $C_{\hat{F}_y}$ exhibits a positive value as the front part of the tornado hits the building first and pushes it in the positive *y* direction. As the trailing portion of the tornado encounters the building, the wind blows from the opposite direction and produces negative values for $C_{\hat{F}_y}$. $C_{\hat{F}_z}$ exhibits only upward forces. This is consistent with the concept that the primary cause of $C_{\hat{F}_z}$ in this case is the negative pressure region that develops within a large vortex.

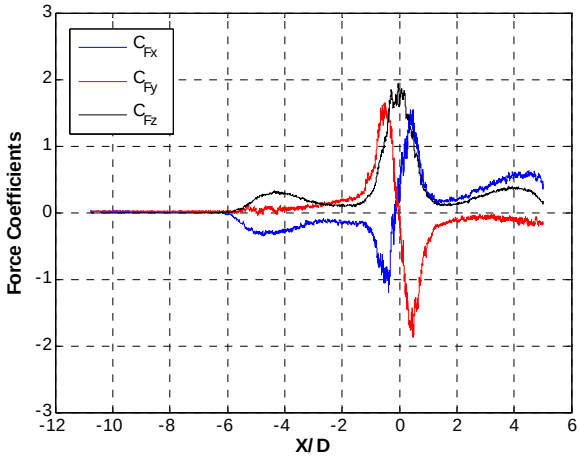

Figure 2: Typical plots of force coefficients on a building model with respect to tornado position (x) referenced to the center of the building model.

4 PARAMETER STUDY

4.1 Single Building Model in a Range of Tornado Sizes

A study was conducted using a range of tornado vortices on a single building 35° gable roof building model. The model was exposed to tornadoes of five different radii referred to as cases "Vane 1" to "Vane 5" (corresponding to vortex radii of 0.23m through 0.53m). The building orientation angle, θ (see Fig. (1)) was varied between 0° and 90°. In addition, for each tornado and building angle, the vortex translation speed was varied between 0.15m/s and 0.61m/s. This test matrix consisted of 140 cases. Each case was repeated 10 times to reduce precision uncertainty.

To summarize the results of this study, peak force coefficients were calculated by identifying the peak positive and negative values of each test (for example, see Fig. (2)). For each case, the peak values for 10 runs were averaged to estimate a peak force coefficient. Figs. (3), (4) and (5) show the peak force coefficients, $C_{\hat{F}_x}$ (the hat in the subscript denotes a peak quantity) for the x, y and z directions, respectively. The peak values for all 140 test cases are shown.

In each of these plots, there are two sets of data. The open symbols represent the peak force coefficients measured in the lab and normalized by the maximum average tangential velocity in the tornado simulator. These "model" coefficients could be referred to as $C_{\hat{F}_m}$ and are normalized by $V_{\theta_{\max}}$ (see the left side of Eqn. (2)). To make a reasonably consistent comparison with ASCE 7-05 wind load provisions, however, it was necessary to normalize the peak force values with peak velocity values and generate "full scale" coefficients, $C_{\hat{F}_{fs}}$, which are normalized by a peak velocities, $\hat{V}_{\theta_{\max}}$ (as shown in the right side of Eqn. (2)). For this study, these peak velocities were estimated using mean velocities, time scales and gust factor curves. In the future, the peak velocities will be determined directly from turbulence measurements in the simulator.

$$C_{\hat{F}_m} = \frac{\hat{F}_m}{\frac{1}{2}\rho V_{\theta_{\max}}^2 S_m} \quad \Rightarrow \quad C_{\hat{F}_{fs}} = \frac{\hat{F}_{fs}}{\frac{1}{2}\rho \hat{V}_{\theta_{\max}}^2 S_{fs}} \tag{2}$$

ASCE 7-05 values were also computed for this building model using Method 2 for the Main Wind Force Resisting System (MWFRS) and assuming a geometric scale of 1:100. The wind directionality factor, K_d, was assumed to 1.0.

Certain trends are evident in the data. First, the peak values decrease as translation speed increases. It is possible that some of this translation speed dependence results from a tilting of the vortex as it translates. Flow visualization shows evidence for some tilting.

For $C_{\hat{F}_x}$, building orientations of 0° and 90° showed the largest peak force values while intermediate building orientations of 45°, 60° and 75° generally showed larger peak magnitudes for $C_{\hat{F}_y}$. $C_{\hat{F}_z}$ did not show any significant trend with respect to building orientation.

In addition to the above, tornadoes of smaller diameter were found to produce larger peak load coefficients. These smaller diameter vortices have a smaller swirl ratio and thus are somewhat tighter and more organized.

The experimental values for peak load coefficients for $C_{\hat{F}_x}$ and $C_{\hat{F}_y}$ were rather similar to ASCE 7-05 coefficients. In some cases, however, the tornado-induced coefficients were larger than code values. In the case of $C_{\hat{F}_z}$, the experimental values were consistently larger than the code's provisions. These comparisons represent only a first step in comparing tornado-induced loading with straight-line wind loading. The code values were, of course, derived from straight-line wind data, so direct comparisons are not possible. These comparisons should be considered to be a step on the road to a more formal representation of tornado-induced wind loading.

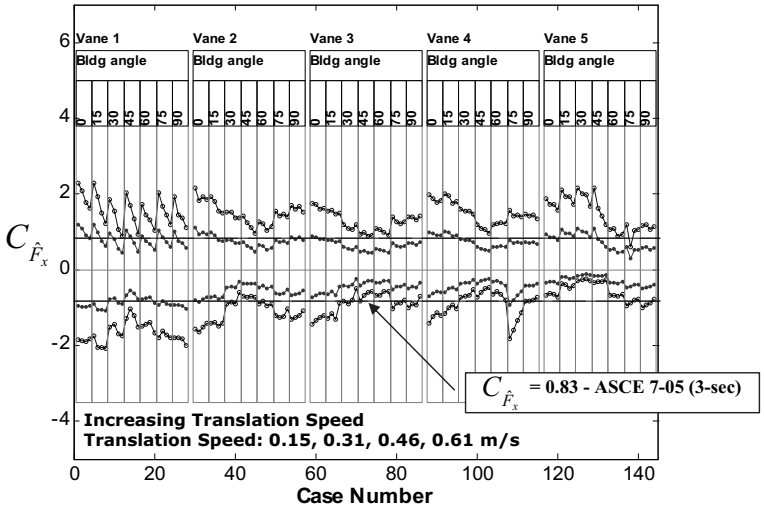

Figure 3: Maximum and minimum $C_{\hat{F}_x}$ for a 35° gable roof building. The four values within each column represent the four translation speeds. Open symbols represent model-scale coefficients; filled symbols represent full-scale coefficients.

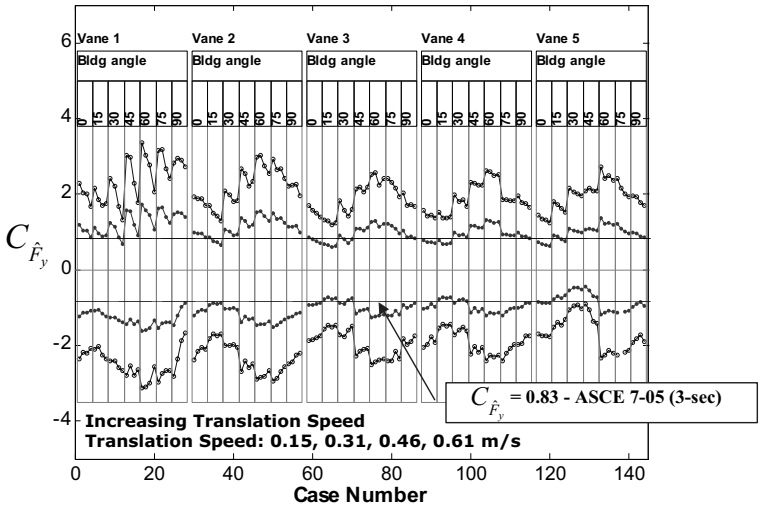

Figure 4: Maximum and minimum $C_{\hat{F}_y}$ for a 35° gable roof building. The four values within each column represent the four translation speeds. Open symbols represent model-scale coefficients; filled symbols represent full-scale coefficients.

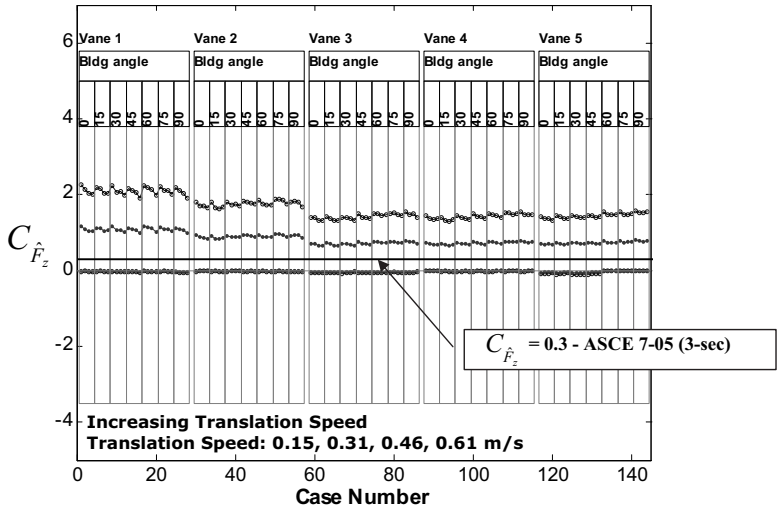

Figure 5: Maximum and minimum $C_{\hat{F}_z}$ for a 35° gable roof building. The four values within each column represent the four translation speeds. Open symbols represent model-scale coefficients; filled symbols represent full-scale coefficients.

4.2 Single Tornado with a Range of Building Geometries

A second set of tests was carried out with several building models being subjected to a single tornado. In this case, the tornado was the "Vane 1" case—the smallest diameter vortex we have and one that generated the largest loading reported in Section 4.1. Figs. (6), (7) and (8) show $C_{\hat{F}_x}$, $C_{\hat{F}_y}$ and $C_{\hat{F}_z}$ for a range of roof types at three building orientation angles at three different vortex translation speeds. $C_{\hat{F}_x}$ values did not show a strong dependence on roof geometry, but $C_{\hat{F}_y}$ did show some tendency for lower peak loads for the hip roof and 15° gable roof. In addition, $C_{\hat{F}_x}$ values did not vary greatly between 1-story and 2-story models, but $C_{\hat{F}_y}$ did increase for 2-story tests compared with 1-story tests. In all cases, $C_{\hat{F}_z}$ did not show significant dependence on either roof geometry or building orientation angle.

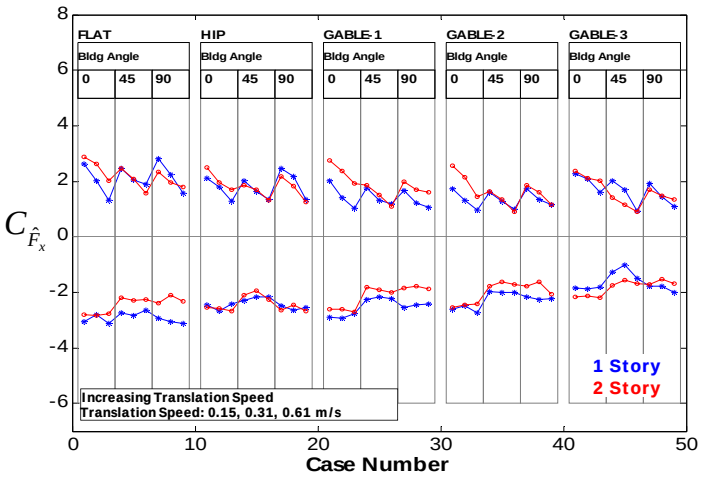

Figure 6: Maximum and minimum $C_{\hat{F}_x}$ for several different roof geometries and two different building heights. The three values within each column represent the three translation speeds.

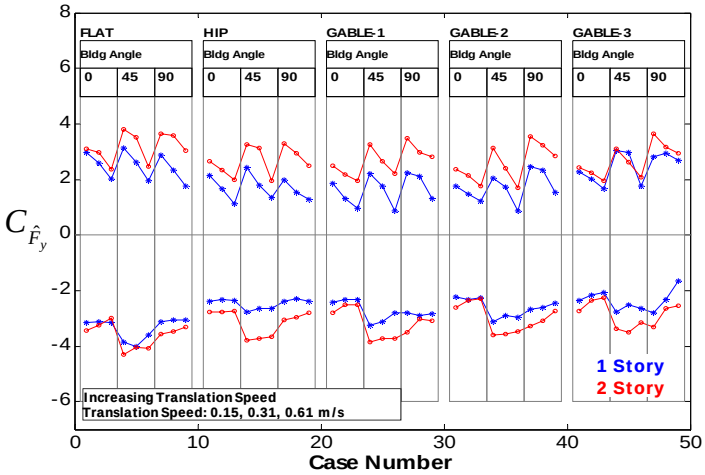

Figure 7: Maximum and minimum $C_{\hat{F}_y}$ for several different roof geometries and two different building heights. The three values within each column represent the three translation speeds.

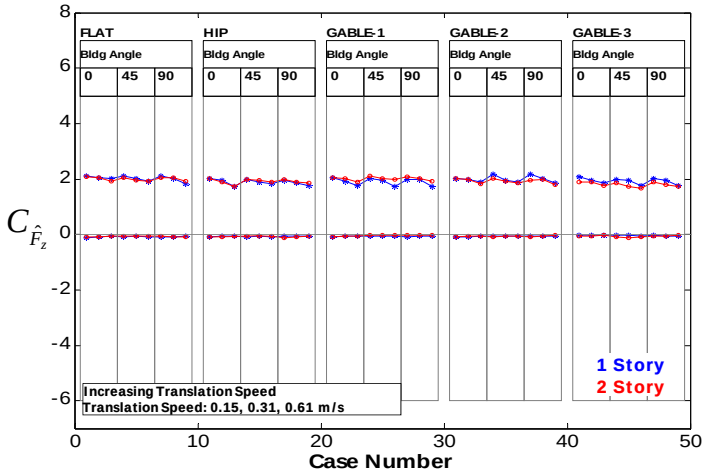

Figure 8: Maximum and minimum $C_{\hat{F}_z}$ for several different roof geometries and two different building heights. The three values within each column represent the three translation speeds.

5 CONCLUSIONS

This investigation of tornado-induced wind loading produced the following observations:

- Lower vortex translation speeds produced higher peak force magnitudes.
- For $C_{\hat{F}_x}$, building orientations of 0° and 90° showed the largest peak force values.
- For $C_{\hat{F}_y}$, building orientations of 45°, 60° and 75° generally showed larger peak magnitudes than the other orientations.
- $C_{\hat{F}_z}$ did not show any significant trend with respect to building orientation.

- Tornadoes of smaller diameter tended to produce larger peak load coefficients.
- Comparing 1-story to 2-story peak coefficients, 2-story coefficients were larger for $C_{\hat{F}_y}$ but were about the same for $C_{\hat{F}_z}$.
- In general, peak force coefficients were found to be similar to the provisions of ASCE 7-05. However, in some cases the tornado-induced coefficients were somewhat larger.

ACKNOWLEDGEMENTS

The authors gratefully acknowledge the support of the National Science Foundation (CMS 0220006), the work of Bill Rickard and numerous undergraduate students from the ISU Aerospace Engineering Department who contributed to this project.

REFERENCES

[1] F.L. Haan, Jr., P.P. Sarkar, W.A. Gallus. Design, construction and performance of a large tornado simulator for wind engineering applications. *Engineering Structures*, **30**, 4, 1146-1159, 2008.

[2] J. Wurman, Personal communication (2004).